NANO LETTERS

Letter

pubs.acs.org/NanoLett

Fast and Efficient Photodetection in Nanoscale Quantum-Dot Junctions

Ferry Prins,*[,†,§] Michele Buscema,[†] Johannes S. Seldenthuis,[†] Samir Etaki,[†] Gilles Buchs,[†] Maria Barkelid,[†] Val Zwiller,[†] Yunan Gao,[†,‡] Arjan J. Houtepen,[‡] Laurens D. A. Siebbeles,[‡] and Herre S. J. van der Zant*[,†]

[†]Kavli Institute of Nanoscience, Delft University of Technology, P.O. Box 5046, 2600 GA, Delft, The Netherlands

[‡]Department of Chemical Engineering, Delft University of Technology, Julianalaan 136, 2628 BL Delft, The Netherlands

Supporting Information

ABSTRACT: We report on a photodetector in which colloidal quantum dots directly bridge nanometer-spaced electrodes. Unlike in conventional quantum-dot thin film photodetectors, charge mobility no longer plays a role in our quantum-dot junctions as charge extraction requires only two individual tunnel events. We find an efficient photoconductive gain mechanism with external quantum efficiencies of 38 electrons-per-photon in combination with response times faster than 300 ns. This compact device-architecture may open up new routes for improved photodetector performance in which efficiency and bandwidth do not go at the cost of one another.

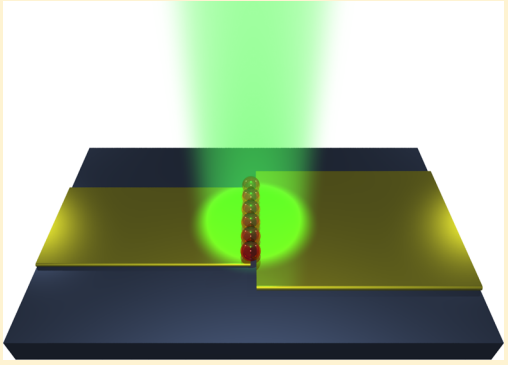

KEYWORDS: *Colloidal quantum dots, nanogap electrodes, nanoscale photodetectors, photoconductive gain*

Colloidal quantum dots (CQDs) profit from the quantum size effect,[1] which gives rise to a variety of unique phenomena such as size tunability, multiexciton processes,[2−4] and slow carrier-relaxation.[5,6] Moreover, they combine low-temperature synthetic methodology with solution processability, allowing for low-cost fabrication methods.[7,8] To date, the use of CQDs as photosensitive material has been mainly focused on thin-film devices.[4,7−9] In these systems, the extraction-efficiencies of photogenerated charges are dominated by the charge mobility, which in CQD-films is generally described by hopping through interparticle barriers. Techniques to enhance the electronic coupling between the CQDs and thus improve the film-mobility include the use of short linkers,[10] various surface passivation approaches[11,12] and the use of CQDs with large Bohr-radii, in particular lead chalcogenide quantum dots. In addition, short channel-length detectors have shown promising performances.[13,14]

An important advancement in the field of quantum-dot photodetectors has been the development of devices capable of photoconductive gain.[7,9] In these devices, exciton generation is followed by the trapping of one of the charge carriers, thereby lowering the chemical potential for transport of the opposite charge carrier. If the trap lifetime exceeds the transit time of the opposite charge carrier, many carriers worth of current can pass through the circuit before recombination takes place. As a consequence, the measured photoconductance is considerably larger than without the presence of such a gain mechanism. This gain in efficiency does, however, go at the expense of an increase in the response time due to the slow trap-state dynamics, which is typically in the order of milliseconds.[7,9]

Here, we present a photodetector which places a one-dimensional parallel array of quantum dots in direct contact with nanometer-separated electrodes (see Figure 1a). In this CQD-junction, charge mobility no longer plays a role as the contact of both source and drain electrodes to each CQD allows for direct charge extraction, which is both fast and efficient.

Nanometer-spaced electrodes are fabricated by a self-aligned fabrication scheme, consisting of a basic two-step lithography process[15−17] (see the Supporting Information for details). An advantage of the self-alignment technique is that the nanometer-separated electrodes can be prepared over large widths, which allows contact to many particles in parallel (see Figure 1b). Here, we use devices with an electrode separation of 4 nm and with an electrode width of 10 μm. A single layer (see the Supporting Information) of PbSe quantum dots of 4 nm in size is placed on top of the electrodes using dipcoating[18] after which a subsequent ligand substitution step with 1,2-ethanedithiol increases the coupling to the electrodes. Electrical contact of the particles to the electrodes is confirmed by performing electrical characterization before and after deposition at room temperature in a vacuum probe station. Before deposition the resistance in all 300 devices studied is >100 GΩ at voltages up

Received: August 13, 2012
Revised: October 15, 2012

   dx.doi.org/10.1021/nl303008y | *Nano Lett.* XXXX, XXX, XXX−XXX

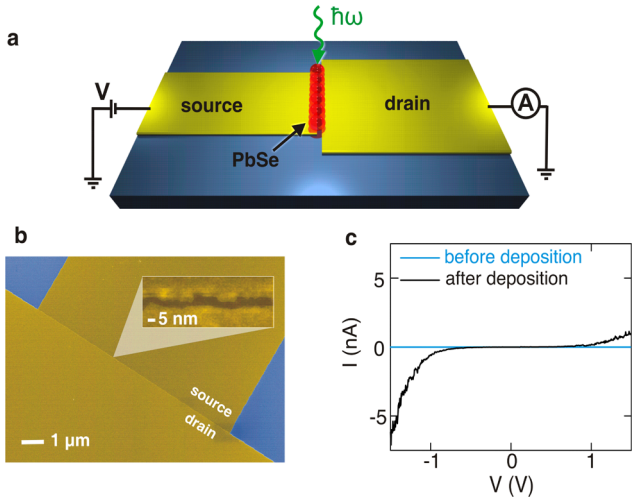

Figure 1. (a) Schematic of the device architecture illustrating the one-dimensional CQD array geometry. (b) Colorized scanning electron micrograph of an empty 10 μm wide device fabricated by a self-aligned fabrication scheme (see methods section). The inset shows a zoom-in of the nanogap area. (c) Room-temperature current–voltage characteristics before and after deposition of PbSe CQDs. The device width is 10 μm. Measurements are performed in a vacuum probe-station at room temperature.

to 2.5 V, whereas after deposition of the PbSe QDs a clear onset of conductance is observed at approximately 1 V, reflecting the density of states inside the dots (see Figure 1c).

In all devices, we found a strong photoconductive effect when irradiating them with visible light. Current–voltage (I–V) characteristics taken under laser light irradiation (λ = 532 nm, and an irradiance of E = 0.16 Wcm^{-2}, see Figure 2a) display a linear dependence with the applied voltage in the low-bias regime; at higher bias the I–V characteristics become nonlinear at the onset of the dark current. Control experiments in which bare nanogaps without PbSe-QDs are illuminated, display no photoconductive response.

To spatially resolve the photoconductive response, we place a device in an optical scanning confocal-microscope setup. While scanning a diffraction limited laser spot (λ = 532 nm, spot size of ~800 nm) across the device, the current is measured as a function of the spot position. Conductance maps, recorded at 750 mV, show a high photoconductive response when the laser spot is placed directly on top of the nanogap area (see Figure 2b, data corrected for the dark current). The response along the gap is consistently above 2 nA, with some variations in the current (within a factor of 2). These variations maybe the result of a nonuniformity in the distribution of PbSe QDs along the gap or in the electronic coupling of the particles to the electrodes. The full width at half-maximum of the photoresponse is 805 nm measured perpendicular to the nanogap, consistent with the spot size of our diffraction-limited laser beam (see Supporting Information).

The photoconductive response depends strongly on the wavelength of the incident light. For the device of Figure 2b, we fix the laser at the position of maximum response and measure the current at V = 750 mV and constant optical power, P = 15 μW, for varying wavelengths between 850 nm and 1650 nm as shown in Figure 2c. The spectral dependence of the photoconductance closely resembles the absorption spectrum of a reference film of the same PbSe QDs on quartz (gray solid

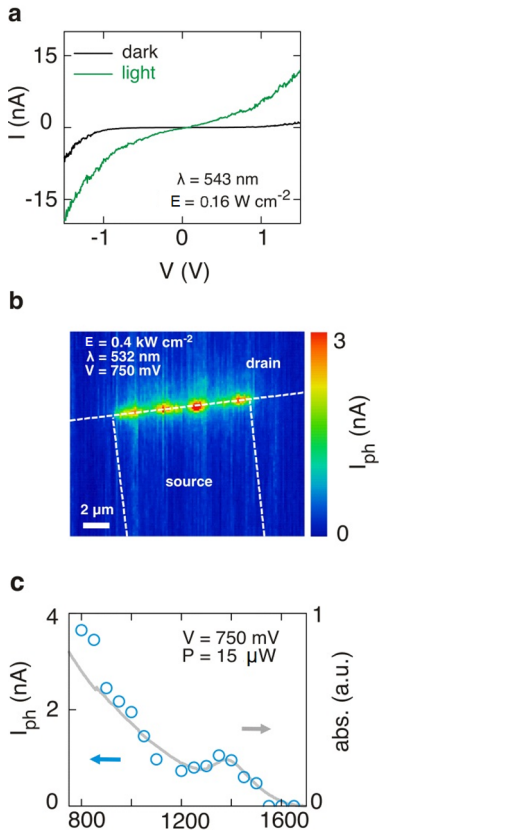

Figure 2. (a) I–V characteristics in the dark (solid black line) and under laser illumination (solid green line, λ = 543 nm, E = 0.16 W cm^{-2}, spot size = 150 μm.) (b) Map of the photocurrent of a different device (corrected for a dark current of 0.8 nA) as a function of the position of the diffraction-limited spot from a different setup with a spot size of about 800 nm (λ = 532 nm). Dashed white lines indicate the electrode edges determined from the reflection image. (c) Wavelength dependence of the photocurrent of the device in B at constant laser power (blue open circles). Photocurrent points are taken at a fixed position of maximum response of the device. The optical absorption spectrum of a solid film of CQDs (solid gray line) is shown for comparison.

line in Figure 2c), including the peak absorption at the bandgap energy and the absence of response at longer wavelengths (λ > 1600 nm). The correspondence to the QD's absorption spectrum shows that the photoconductance is driven by optical excitations inside the QDs.

We have also recorded the photocurrent at λ = 532 nm at different optical powers (between E = 2 and 2000 W cm^{-2}, shown in Figure 3a). At low powers (E < 50 W cm^{-2}), the current scales linearly with the laser power, while at higher powers (E > 50 W cm^{-2}) the current saturates. We attribute the saturation at high powers to the filling of trap states which reduces the efficiency to the photoconductance gain mechanism, as is discussed below. At lower powers the efficiency is highest. The external quantum efficiency (EQE), that is, the number of extracted electrons (or holes) per photon incident on the device, can be calculated with

$$\mathrm{EQE} = \frac{I_{\mathrm{ph}}}{e}\frac{\hbar\omega}{E \cdot A} \qquad (1)$$

where I_{ph} is photocurrent (corrected for the dark current) and A is the illuminated device area (4 × 800 nm^2). For the device in Figure 3a, the efficiency reaches 10.9 electrons per photon at

dx.doi.org/10.1021/nl303008y | Nano Lett. XXXX, XXX, XXX–XXX

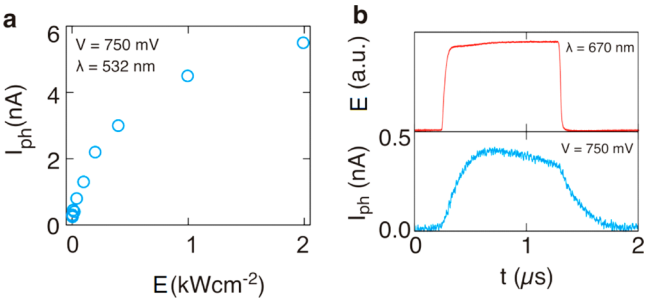

Figure 3. (a) Photocurrent as a function of irradiance (blue open circles, corrected for the dark current) for the device in Figure 2b and c. (b) Photocurrent response (bottom panel, corrected for the dark current) of a different device to a 1 μs square pulsed laser illumination (top panel, λ = 670 nm, E = 0.85 W cm^{-2}, spot size = 150 μm). The rise and fall time of the laser signal is <20 ns.

2 W cm^{-2} with a bias of 750 mV (see Supporting Information). At higher bias the photon-to-electron conversion is even more efficient; for example in the $I-V$ characteristic of Figure 2a, which is taken at low power; an EQE of 38 electrons per photon is observed at a bias of 1.5 V. In the calculation of the EQE it is assumed that all light incident on the gap area is absorbed by the one-dimensional array of quantum dots. If we do take the absorption probability of the single row of CQDs into account,[19] we can determine the internal quantum efficiency (IQE) of the detector. Assuming a coverage of 2000 4-nm-sized particles across the 10 μm wide device of Figure 2a, we obtain IQEs as high as 5.9 × 10^3 electrons per photon (see Supporting Information).

The most striking feature of our device performance is the combination of high efficiency with fast response. Figure 3b shows the temporal photoresponse of the device to a 1 μs laser pulse, measured using a low-noise amplifier and a 600 MHz oscilloscope. The observed rise and fall time of our device are approximately 200 and 300 ns, respectively, limited by the electronic bandwidth of the measurement circuit (see Supporting Information). Such fast response times combined with high efficiencies are crucial parameters in, for instance, video-rate laser-scanning microscopy where dwell-times in the order of 100 ns are required.[20]

High efficiencies in CQD-photodetectors are usually achieved by trapping of one of the charge carriers, which is photoinduced by the incident light. The trapping of charge carrier lowers the chemical potential for transport of the opposite charge carrier, thereby increasing the conductance.[8] If the lifetime of the trap state exceeds the carrier transit-time, several opposite charge carriers can pass through the device before recombination with the trapped charge occurs. Thus, instead of the charge carriers that originate from the exciton pair only, many more charge carriers contribute to the photoconductance. The gain factor in this picture is proportional to the ratio of the trap lifetime over the transit time. For conventional film-based CQD photoconductors, which have typical mobilities between 10^{-1} and 10^{-3} cm^2 V s^{-1} and channel lengths of around a micrometer, the transit time is hundreds of nanoseconds or longer.[12,13] Appreciable gain therefore requires trap-state life times as long as milliseconds, inevitably leading to the slow response times of these devices.

The orders-of-magnitude shorter rise and fall time of our device shows that, if trap-induced photoconductive gain is responsible for the high efficiency, the mechanism needs to be active on very short time scales. This would first of all require short-lived trap states, shorter than the observed 200 and 300 ns rise and fall time, and second, it would require subnanosecond transit times to explain the observed IQE. Short transit times are indeed feasible in our device as a direct result of the nanoscale geometry: the transit time is determined by the product of the tunnelling probabilities of the two barriers that separate each CQD from source and drain. The interfacial electronic coupling energy for PbSe CQDs at or near resonance is reported to be as high as 100 meV,[21] corresponding to individual tunnel events at subpicosecond time scales.[6] Taking this into consideration, even short-lived traps ($\ll$ 200 ns) could thus lead to considerable gain factors in our device, allowing for high efficiency at short time scales.

For a possible explanation for the short-lived trap states we take a closer look at the quantum dot junction. With the CQD only separated from source and drain by two tunnel barriers, the stochastic nature of the individual charge extraction events becomes important.[22−24] After creation of an exciton, either the electron or the hole will be extracted first, leaving the opposite carrier temporarily behind as if it was trapped. If it is for instance the hole which is left behind, the chemical potential for transport of electrons through the dot is brought closer into resonance with the Fermi level as a result of the reduced Coulombic repulsion. This leads to photoconductive gain in the same way as a conventional trap state at for instance the surface of a quantum dot would.[25] The crucial difference with conventional traps is, however, that the lifetime of the trap is only determined by the probabilistic nature of the tunnel events, which occur at the before mentioned subpicosecond time-scales.[6,21]

In the above discussion we have not taken into account plasmonic field enhancement effects that are known to increase light collection in nanogapped structures (i.e., enlarge the optical cross-section of the dots).[26−30] If present, they would also contribute to the enhancement of the IQE number so that the gain is not solely determined by the ratio of the trap lifetime over the transit time.

In conclusion, the presented architecture offers a promising route toward solution processable, low-cost, nanoscale devices with ultrafast yet efficient detection performance. It moreover comprises a versatile platform to study the microscopic details of charge transfer at the metallic interface, not limited to colloidal quantum dots only, but applicable to a variety of nanomaterials. In addition, we expect that plasmonic field enhancement may already play a role in the efficiency of our device, although the effect is expected to be small for the broad nonresonant electrodes we have used in our experiment. It will therefore be interesting to investigate devices with smaller widths which could profit from both efficient carrier extraction, as well as optimized light absorption by resonant plasmonic field enhancement.

■ ASSOCIATED CONTENT

Supporting Information

Experimental details, additional device characterization, and bandwidth analysis. This material is available free of charge via the Internet at http://pubs.acs.org.

■ AUTHOR INFORMATION

Corresponding Author

*E-mail: (F.P.) prins@mit.edu; (H.vd.Z.) h.s.j.vanderzant@tudelft.nl.

dx.doi.org/10.1021/nl303008y | Nano Lett. XXXX, XXX, XXX−XXX

Present Address
[§]Department of Chemical Engineering, Massachusetts Institute of Technology, 77 Massachusetts Avenue, Cambridge, Massachusetts 02139, United States.

Notes
The authors declare no competing financial interest.

■ ACKNOWLEDGMENTS

We thank G. A. Steele, J. M. Thijssen, Y. M. Blanter, R. W. Heeres, and W. A. Tisdale for discussions. We thank M. van Oossanen, R. Schouten, and R. van Ooijik for technical assistance. This work was supported by Stichting FOM under the programs 86 and 111 and a FOM projectruimte, through the FP7-framework program ELFOS and a Marie Curie Intra European Fellowship (G.B.).

■ REFERENCES

(1) Brus, L. E. *J. Chem. Phys.* **1984**, *80* (9), 4403−4409.
(2) Beard, M. C. *J. Phys. Chem.Lett.* **2011**, *2* (11), 1282−1288.
(3) Schaller, R. D.; Klimov, V. I. *Phys. Rev. Lett.* **2004**, *92* (18), 186601.
(4) Sukhovatkin, V.; Hinds, S.; Brzozowski, L.; Sargent, E. H. *Science* **2009**, *324* (5934), 1542−1544.
(5) Pandey, A.; Guyot-Sionnest, P. *Science* **2008**, *322* (5903), 929−932.
(6) Tisdale, W. A.; Williams, K. J.; Timp, B. A.; Norris, D. J.; Aydil, E. S.; Zhu, X. Y. *Science* **2010**, *328* (5985), 1543−1547.
(7) Konstantatos, G.; Howard, I.; Fischer, A.; Hoogland, S.; Clifford, J.; Klem, E.; Levina, L.; Sargent, E. H. *Nature* **2006**, *442* (7099), 180−183.
(8) Konstantatos, G.; Sargent, E. H. *Nat. Nanotechnol.* **2010**, *5* (6), 391−400.
(9) Lee, J. S.; Kovalenko, M. V.; Huang, J.; Chung, D. S.; Talapin, D. V. *Nat. Nanotechnol.* **2011**, *6* (6), 348−352.
(10) Yu, D.; Wang, C. J.; Guyot-Sionnest, P. *Science* **2003**, *300* (5623), 1277−1280.
(11) Liu, Y.; Gibbs, M.; Perkins, C. L.; Tolentino, J.; Zarghami, M. H.; Bustamante, J.; Law, M. *Nano Lett.* **2011**, *11* (12), 5349−5355.
(12) Tang, J.; Kemp, K. W.; Hoogland, S.; Jeong, K. S.; Liu, H.; Levina, L.; Furukawa, M.; Wang, X. H.; Debnath, R.; Cha, D. K.; Chou, K. W.; Fischer, A.; Amassian, A.; Asbury, J. B.; Sargent, E. H. *Nat. Mater.* **2011**, *10* (10), 765−771.
(13) Hegg, M. C.; Horning, M. P.; Baehr-Jones, T.; Hochberg, M.; Lin, L. Y. *Appl. Phys. Lett.* **2010**, *96* (10), 101118.
(14) Willis, L. J.; Fairfield, J. A.; Dadosh, T.; Fischbein, M. D.; Drndic, M. *Nano Lett.* **2009**, *9* (12), 4191−4197.
(15) Fursina, A.; Lee, S.; Sofin, R. G. S.; Shvets, I. V.; Natelson, D. *Appl. Phys. Lett.* **2008**, *92* (11), 113102.
(16) Prins, F.; Monrabal-Capilla, M.; Osorio, E. A.; Coronado, E.; van der Zant, H. S. J. *Adv. Mater.* **2011**, *23* (13), 1545−1549.
(17) Tang, J.; De Poortere, E. P.; Klare, J. E.; Nuckolls, C.; Wind, S. J. *Microelectron. Eng.* **2006**, *83* (4−9), 1706−1709.
(18) Talgorn, E.; Gao, Y. N.; Aerts, M.; Kunneman, L. T.; Schins, J. M.; Savenije, T. J.; van Huis, M. A.; van der Zant, H. S. J.; Houtepen, A. J.; Siebbeles, L. D. A. *Nat. Nanotechnol.* **2011**, *6* (11), 733−739.
(19) Moreels, I.; Lambert, K.; De Muynck, D.; Vanhaecke, F.; Poelman, D.; Martins, J. C.; Allan, G.; Hens, Z. *Chem. Mater.* **2007**, *19* (25), 6101−6106.
(20) Saar, B. G.; Freudiger, C. W.; Reichman, J.; Stanley, C. M.; Holtom, G. R.; Xie, X. S. *Science* **2010**, *330* (6009), 1368−1370.
(21) Tisdale, W. A.; Zhu, X. Y. *Proc. Natl. Acad. Sci. U.S.A.* **2011**, *108* (3), 965−970.
(22) Galperin, M.; Nitzan, A. *Phys. Chem. Chem. Phys.* **2012**, *14* (26), 9421−9438.
(23) Wang, L. X.; May, V. *Chem. Phys.* **2010**, *375* (2−3), 252−264.
(24) Wang, L. X.; May, V. *J. Electroanal. Chem.* **2011**, *660* (2), 320−331.
(25) We note that, although conventional surface trap states could still be present, our results show they are either short-lived (<200−300 ns), or have negligible effect on the photocurrent.
(26) Im, H.; Bantz, K. C.; Lindquist, N. C.; Haynes, C. L.; Oh, S. H. *Nano Lett.* **2010**, *10* (6), 2231−2236.
(27) Ishi, T.; Fujikata, J.; Makita, K.; Baba, T.; Ohashi, K. *Jpn. J. Appl. Phys.* **2005**, *44* (12−15), L364−L366.
(28) Miyazaki, H. T.; Kurokawa, Y. *Phys. Rev. Lett.* **2006**, *96* (9), 097401.
(29) Shi, S. F.; Xu, X. D.; Ralph, D. C.; McEuen, P. L. *Nano Lett.* **2011**, *11* (4), 1814−1818.
(30) Ward, D. R.; Halas, N. J.; Ciszek, J. W.; Tour, J. M.; Wu, Y.; Nordlander, P.; Natelson, D. *Nano Lett.* **2008**, *8* (3), 919−924.